Review

A Short Review: Comparison of Zinc–Manganese Dioxide Batteries with Different pH Aqueous Electrolytes

Ramona Durena * and Anzelms Zukuls

Institute of Materials and Surface Engineering, Faculty of Materials Science and Applied Chemistry, P. Valdena 3/7, LV-1010 Riga, Latvia; anzelms.zukuls@rtu.lv
* Correspondence: ramona.durena@rtu.lv

Abstract: As the world moves towards sustainable and renewable energy sources, there is a need for reliable energy storage systems. A good candidate for such an application could be to improve secondary aqueous zinc–manganese dioxide ($Zn\text{-}MnO_2$) batteries. For this reason, different aqueous $Zn\text{-}MnO_2$ battery technologies are discussed in this short review, focusing on how electrolytes with different pH affect the battery. Improvements and achievements in alkaline aqueous $Zn\text{-}MnO_2$ batteries the recent years have been briefly reviewed. Additionally, mild to acidic aqueous electrolyte employment in $Zn\text{-}MnO_2$ batteries has been described, acknowledging their potential success, as such a battery design can increase the potential by up to 2 V. However, we have also recognized a novel battery electrolyte type that could increase even more scientific interest in aqueous $Zn\text{-}MnO_2$ batteries. Consisting of an alkaline electrolyte in the anode compartment and an acidic electrolyte in the cathode compartment, this dual (amphoteric) electrolyte system permits the extension of the battery cell potential above 2 V without water decomposition. In addition, papers describing pH immobilization in aqueous zinc–manganese compound batteries and the achieved results are reported and discussed.

Keywords: Zn anode; MnO_2 cathode; energy storage; dual electrolyte; amphoteric electrolyte; anolyte; catholyte

1. Introduction

Effective and reliable battery technology is highly desired as the world leans toward sustainable energy sources, such as hydro, solar, and wind energies. However, all these options suffer from uneven energy production patterns throughout the day and year and cannot supply the energy on demand [1]. One way to overcome these shortcomings is to store the excess energy in batteries or create more everyday appliances with accumulators. This would allow us to charge up these devices when energy is available, such as in the daytime, from solar panels and use electricity-powered devices in the evening [2].

Li-ion batteries (LIBs) in recent decades have found wide applications in consumer electronics [3], such as computers, cell phones [4], and now also electric and hybrid vehicles [5]. The extensive use of LIBs can be attributed to their high energy density (up to 500 Wh/L), power density (up to 300 W/kg), high theoretical lithium storage capacity (890 mA h/g), operating voltage (>3.7 V), excellent cycling performance (over 10,000 cycles), and low self-discharge (<5% of the stored capacity over 1 month) [6–9]. However, the optimal operating range of LIBs is 15–35 °C. Furthermore, battery overheating can induce the melting of the separator, which causes an internal short circuit. In this short-circuit spot, a rapid self-heating begins at a rate of around 2592.0 to 11,860.0 °C min^{-1} [10], resulting in a thermal runaway [11,12]. This means that once the process has started, no cooling application can stop it. Unfortunately, this process results in a fire or an explosion, thus creating a considerable safety risk for consumers [4,13,14]. Furthermore, another significant drawback has emerged: a material shortage of commonly used metals in LIBs could be on the rise [15–17]; thus, this suggests that new or improved battery technology is needed.

One such technology could be improved aqueous Zn-MnO$_2$ batteries. They do not pose large safety risks; the two-electron reaction of Zn^{2+}/Zn has a high theoretical capacity of 820 mAh/g, Zn has low toxicity, and is earth-abundant [18,19]. Moreover, MnO$_2$ as a cathode has an attractive total theoretical capacity of 617 mAh/g. Thus, making Zn-MnO$_2$ cells with an energy density of >400 W h/L and >500 Wh/kg [20], which is comparable to some LIBs, is an interesting technology to improve large-scale rechargeable battery applications.
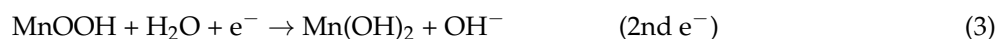
The origin of aqueous Zn-MnO$_2$ batteries can be traced back to 1866 when the French scientist Georges-Lionel Leclanché created and patented the first Zn-MnO$_2$ battery, which was called the Leclanché cell [21]. Improving the electrolyte composition and design of this battery cell has led to the creation of commercialized dry cells. Further development of Zn-MnO$_2$ batteries took place in the 1950s when the Canadian engineer Lewis Urry improved and rebuilt the battery cell known at that time. In 1960, a patent was granted for aqueous alkaline Zn-MnO$_2$ batteries [22–24]. These batteries have continued their development until now, improving the composition and shelf life, and replacing harmful elements inside the batteries, such as mercury. This has led aqueous alkaline Zn-MnO$_2$ batteries to be the longest and most widely used primary battery technology that still dominates the global market as the primary battery source nowadays [25].

Aqueous alkaline Zn-MnO$_2$ batteries consist of a zinc metal anode, a manganese dioxide powder mixture with finely dispersed carbon as the cathode, and concentrated potassium hydroxide (>30 wt%) aqueous solution as the electrolyte. In this electrode pairing (as depicted in Figure 1), Zn acts as an anode with a standard potential of −1.199 V vs. SHE (standard hydrogen electrode) and undergoes reaction (1), whereas MnO$_2$ acts as an active material in the cathode with a standard potential of +0.250 V vs. SHE and undergoes reactions (2) and (3) in the primary cells. As MnO$_2$ is non-conductive, usually a small amount of finely dispersed carbon is added to ensure the conductivity of the cathode. This results in an overall reaction (4) [1,26–28]. The calculated open circuit potential (OCP) for this system of 1.45 V is in discrepancy with the actual commercially available battery OCP of 1.55–1.6 V. This effect can be attributed to the fact that reactions (1)–(4) are very general and the actual system is quite complex [29–32]. Additionally, the total theoretical capacity of the MnO$_2$ cathode consists of a two-stage (two-electron) reaction. The first electron reaction (2) of the MnO$_2$ cathode in an alkaline medium corresponds to the intercalation of hydrogen in the solid phase with a theoretical capacity of 309 mAh/g. As the discharge continues, the second electron reaction (3) can also occur. A dissolution–precipitation heterogeneous process with a theoretical capacity of 308 mAh/g continues to enter the deep discharge stage of the cathode [20,28,33].
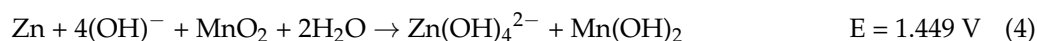
Anode:

$$Zn + 4(OH)^- \rightarrow Zn(OH)_4{}^{2-} + 2e^- \qquad\qquad E^0 = -1.199 \text{ V vs. SHE} \qquad (1)$$

Cathode:

$$MnO_2 + H_2O + e^- \rightarrow MnOOH + OH^- \qquad (1\text{st } e^-) \qquad E^0 = +0.250 \text{ V vs. SHE} \quad (2)$$

$$MnOOH + H_2O + e^- \rightarrow Mn(OH)_2 + OH^- \qquad (2\text{nd } e^-) \qquad\qquad (3)$$

Overall:

$$Zn + 4(OH)^- + MnO_2 + 2H_2O \rightarrow Zn(OH)_4{}^{2-} + Mn(OH)_2 \qquad\qquad E = 1.449 \text{ V} \quad (4)$$

Although researched for a very long time now, alkaline Zn-MnO$_2$ batteries are still of great interest to scientists. Aqueous alkaline electrolyte Zn-MnO$_2$ batteries have proven to be a great source for primary batteries; however, their secondary battery performance is very limited due to the formation of insoluble compounds (usually in the second electron reaction of the cathode). For this reason, many scientists are devoting their research activi-

ties to developing rechargeable aqueous Zn-MnO$_2$ secondary batteries with higher specific capacities and OCP. In this short review, we discuss improvements and achievements in recent years for different aqueous Zn-MnO$_2$ battery types, as shown in Figure 2. We have discussed alkaline and acidic/mild aqueous electrolyte rechargeable Zn-MnO$_2$ battery types and also recognized a dual (amphoteric) aqueous electrolyte battery concept that could increase research interest in aqueous Zn-MnO$_2$ batteries.
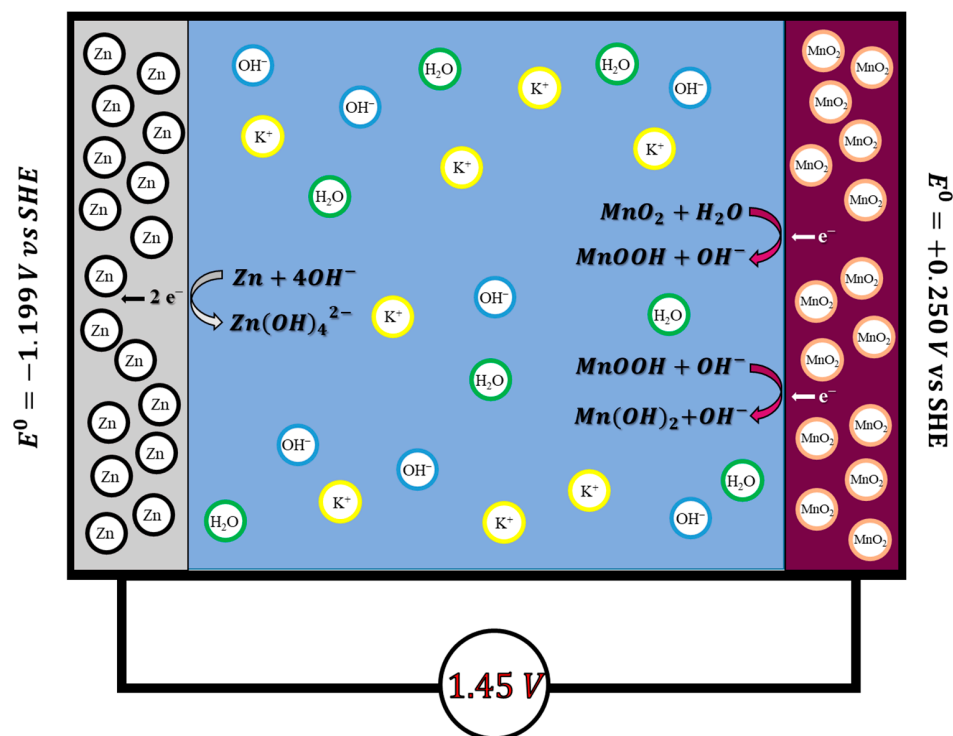

Figure 1. The schematic working mechanism of alkaline Zn-MnO$_2$ batteries.
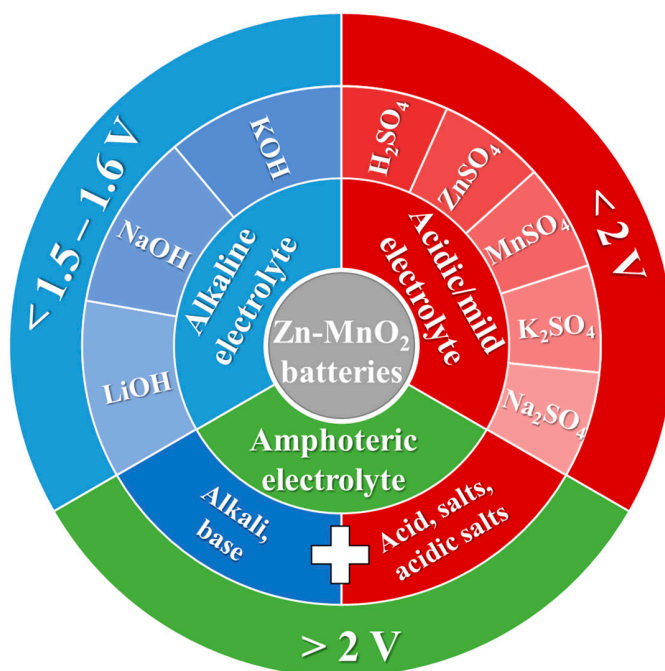

Figure 2. Different types of Zn-MnO$_2$ batteries with their possible potentials and the most commonly used electrolytes.

2. Alkaline Electrolyte Zn-MnO$_2$ Batteries

Many authors have attributed the poor rechargeability of alkaline Zn-MnO$_2$ batteries to the formation of electrochemically inactive manganese oxides such as Mn$_3$O$_4$ and ZnMn$_2$O$_4$. These oxides form during deep discharge that takes place while accessing the second electron capacity of MnO$_2$ [22,34]. After several charge/discharge cycles, the irreversible manganese oxides coated the active MnO$_2$ particles, preventing them from undergoing further reactions. N. D. Ingale with co-authors [35] investigated this problem and provided proof for the connection between insoluble compound formation and the depth of discharge (DOD). They experimentally obtained 3000 cycles for alkaline (45 wt% KOH water solution) Zn-MnO$_2$ batteries at 10% DOD. However, at 20% DOD, only ~500 cycles could be obtained. For these experiments, the DOD was based on the first theoretical electron capacitance of the MnO$_2$ cathode (308 mAh/g).

Other scientists have tried to improve the rechargeability of aqueous alkaline Zn-MnO$_2$ batteries by using additives to electrolytes and/or MnO$_2$ cathodes [7,34]. A.M. Bruck with co-workers [36] investigated the effects of Bi$_2$O$_3$ addition to the MnO$_2$ electrode. They found that Bi^{3+} occupies an interstitial position in the layered MnO$_2$ phase—birnessite— limiting the Mn^{3+} ion diffusion in the lattice. Thus, Bi^{3+} promotes the conversion from the MnO$_2$ birnessite phase directly to Mn(OH)$_2$ and prevents Mn$_2$O$_3$ phase formation during the battery charge/discharge process. A similar technique has been employed by G.G. Yadav with co-authors [28]. They used Cu-intercalated birnessite mixed with Bi$_2$O$_3$ as a cathode in alkaline Zn batteries and obtained capacity reversibility (from the second electron capacity of the MnO$_2$ cathode—617 mAh/g) for more than 6000 cycles. However, the tested cathode material contained only ~19% of the active MnO$_2$ material.

Other authors have investigated the possibility of improving the alkaline aqueous Zn-MnO$_2$ battery system by modifying the electrolytes [34,37–39]. For example, B.J. Hertzberg with co-authors [34] researched the effects of mixing KOH electrolyte with LiOH addition. They found that the insertion of lithium or a combined lithium proton is the dominant reduction mechanism for MnO$_2$. This prevents Zn poisoning reactions and increases the battery cycle lifetime up to 60 cycles with negligible capacity loss (cycling around 360 mAh/g). However, despite their rechargeability improvements, aqueous alkaline Zn-MnO$_2$ batteries still have limited applications due to their low cell potential of ~1.4 V. For this reason, other scientists have gone one step ahead and changed the electrolyte even further, excluding hydroxides entirely.

3. Mild to Acidic Electrolyte Zn-MnO$_2$ Batteries

To overcome the low cell potential of 1.4 V and improve the cyclability of aqueous Zn-MnO$_2$ batteries, other scientists have changed the pH of the electrolyte, thus altering the reaction mechanism of the cell (as depicted in Figure 3). This was achieved by replacing standard hydroxide solutions such as KOH, NaOH, and LiOH [27,34,35,40,41] with ZnSO$_4$, MnSO$_4$ (K$_2$SO$_4$; Na$_2$SO$_4$) [42–47] salts, and/or diluted acid (H$_2$SO$_4$) [48,49]. As shown in the Pourbaix diagram of manganese oxide compounds (Figure 4a), at higher pH values, MnO$_2$ goes through a low potential reaction (0.250 V vs. SHE) with the possibility of transforming into electrochemically inactive manganese oxides such as Mn$_3$O$_4$. However, by lowering the pH value well into the acidic medium, the oxygen atom from the MnO$_2$ cathode can combine with the hydrogen ions to create water; thus, Mn^{4+} ions can be reduced to Mn^{2+} and dissolved in an acidic medium without electrochemically inactive manganese oxide creation. Additionally, the reaction potential of the cathode is significantly improved above 1.2 V vs. SHE by placing MnO$_2$ in an acidic medium. On the other hand, this change in the pH of the electrolyte also increases the reaction potential of the Zn anode, which lowers the overall potential of the cell. As seen in the Pourbaix diagram of zinc oxide compounds (Figure 4b), this potential increase is quite notable, from −1.199 V vs. SHE in an alkaline medium to −0.762 V vs. SHE in an acidic medium.
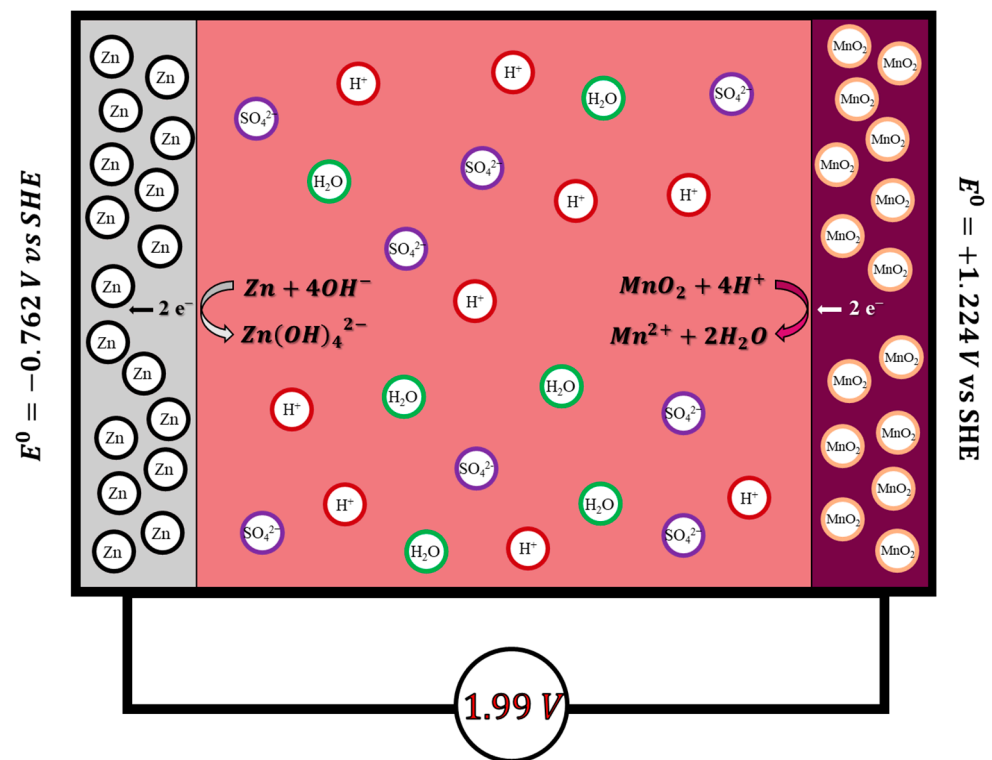
Figure 3. The schematic working mechanism of mild/acidic Zn-MnO$_2$ batteries.
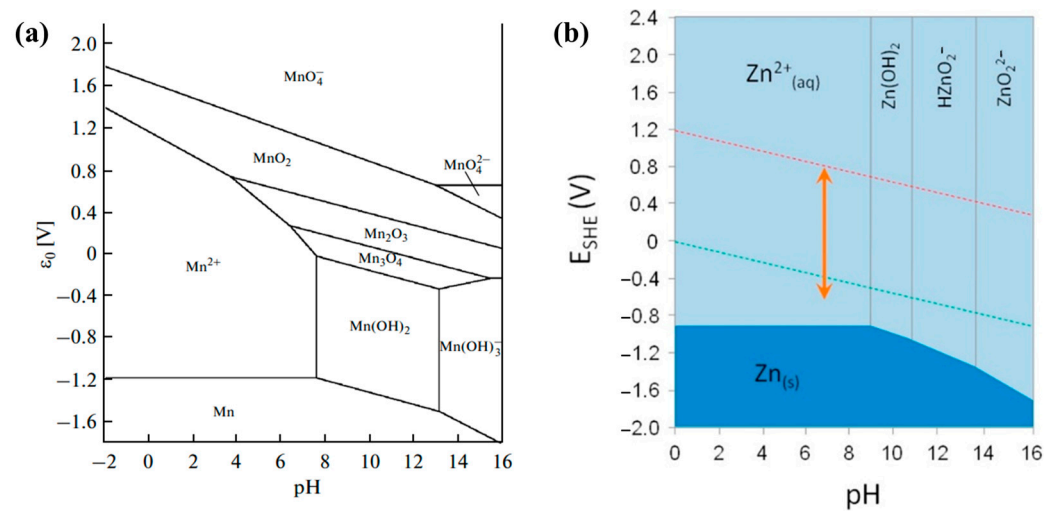

Figure 4. Pourbaix diagram of (**a**) manganese compounds (Reprinted with permission from Ref. [50]; 2015, published by Springer Nature Switzerland AG) and (**b**) zinc compounds in water (Reprinted with permission from Ref. [51]; 2016, published by Elsevier B.V).

Despite the increase in the reaction potential of the Zn anode, this cell configuration allows the cathode to undergo a higher operating potential reaction, resulting in an overall potential increase up to ~2 V, according to reactions (5)–(7) [52]:

Anode:

$$Zn \rightarrow Zn^{2+} + 2e^- \qquad\qquad E^0 = -0.762 \text{ V vs. SHE} \qquad (5)$$

Cathode:

$$MnO_2 + 4H^+ + 2e^- \rightarrow Mn^{2+} + 2H_2O \qquad\qquad E^0 = +1.224 \text{ V vs. SHE} \qquad (6)$$

Overall:

$$Zn + MnO_2 + 4H^+ \rightarrow Zn^{2+} + Mn^{2+} + 2H_2O \qquad\qquad E = 1.986 \text{ V} \quad (7)$$

However, this increased cell potential comes with a considerable drawback. In an acidic environment, a parasitic reaction can take place at the Zn anode. A corrosion reaction can occur, the Zn anode dissociates into the electrolyte as Zn^{2+}, and a hydrogen gas H_2 is produced. This corrosion reaction can not only decrease the capacity but also lead to cell rupture [53]. A. Mitha with co-workers [54] designed Zn-$LiMn_2O_4$ batteries with mildly acidic (pH 4) aqueous electrolyte. To overcome gas production on the anode, fumed silica and polyethylene glycol (MW 300 g/mol) were added. Both additives acted as Zn anode corrosion inhibitors and dendrite suppressors. Thus, this led to achieving a 27–40% lower corrosion current density on the Zn anode and performing 1000 charge–discharge cycles, cycling at a capacity of ~140 mAh/g and retaining ~65% of its initial capacity after 1000 cycles.

H. Pan with co-authors [55] also reported mild electrolyte aqueous Zn-MnO_2 batteries with 5000 charge–discharge cycles and a capacity retention of 92% (based on the first electron capacity of the MnO_2 cathode—308 mAh/g). The high battery cyclability and capacity retention were attributed to the addition of 0.1 M $MnSO_4$ to 2 M $ZnSO_4$ electrolyte. The Mn^{2+} ion suppresses MnO_2 dissolution into the electrolyte, thus improving the stability of the cathode and the utilization of the MnO_2 active material. This idea has been well adapted in the literature [43–46]. However, C. Qiu with co-authors [56] addressed the possibility of adding Mn^{2+} deposition to the MnO_2 cathode while cycling and adding extra capacity to the cathode. Cells with different Mn^{2+} concentrations were tested, and as expected, all the cells showed a stable capacity for a certain number of cycles, followed by fast capacity fading due to the consumption of Mn^{2+} ions from the electrolyte. Although effective for a number of cycles, the Mn^{2+} additive may not be an effective strategy for improving the charge–discharge stability. Furthermore, C. Qiu with co-authors again provided proof for the formation of $ZnMn_2O_4$ at the cathode during discharge, which is attributed to the battery capacity fading and poor cyclability. This indicates that the same rechargeability issues exist in mild aqueous Zn-MnO_2 cells under alkaline conditions. Nonetheless, there could be other methods to improve aqueous Zn-MnO_2 batteries and extend the water decomposition potential window over 1.23 V [57] by combining scientific advances made in aqueous alkaline and acid electrolyte systems.

4. Dual/Amphoteric Electrolyte Zn-MnO$_2$ Batteries

Recently, another type of Zn-MnO_2 battery has been adapted, which takes advantage of the increased MnO_2 potential in acidic electrolytes without creating drawbacks to the Zn anode. This has been realized by placing the Zn anode in an alkaline electrolyte and the MnO_2 cathode in an acidic electrolyte, as shown in Figure 5. By creating such a unique battery cell type, it is possible to increase the OCP to 2.45 V according to reactions (8)–(10) [32,58,59].
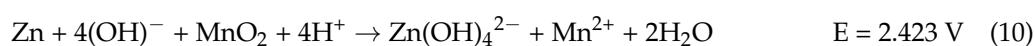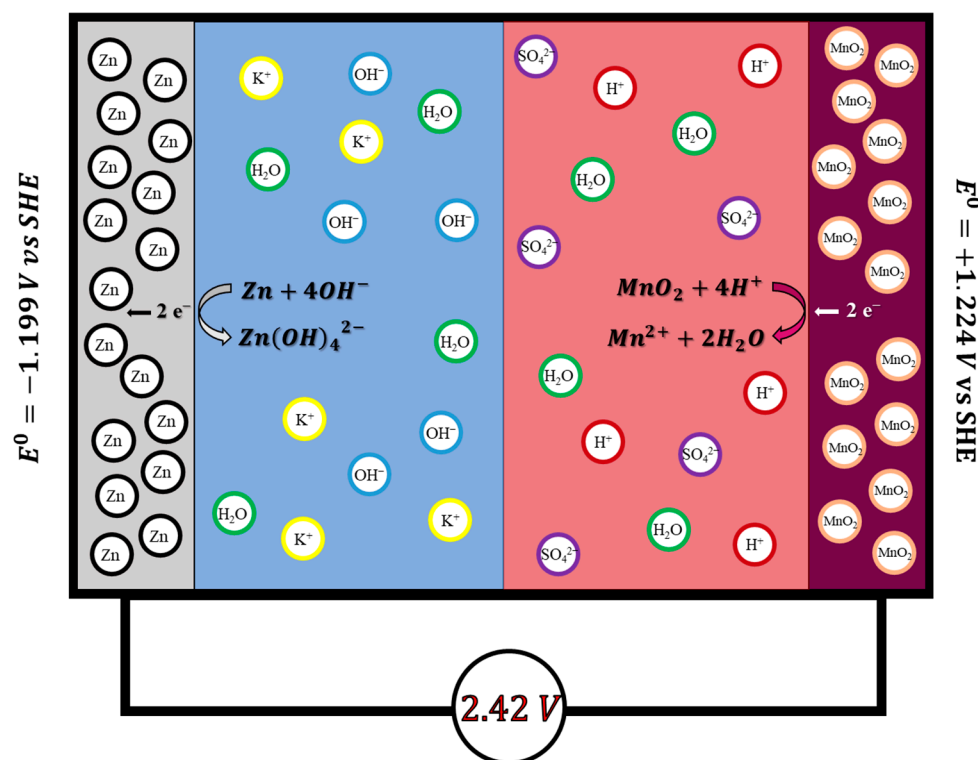
Anode:

$$Zn + 4(OH)^- \rightarrow Zn(OH)_4^{2-} + 2e^- \qquad\qquad E^0 = -1.199 \text{ V vs. SHE} \quad (8)$$

Cathode:

$$MnO_2 + 4H^+ + 2e^- \rightarrow Mn^{2+} + 2H_2O \qquad\qquad E^0 = +1.224 \text{ V vs. SHE} \quad (9)$$

Overall:

$$Zn + 4(OH)^- + MnO_2 + 4H^+ \rightarrow Zn(OH)_4^{2-} + Mn^{2+} + 2H_2O \qquad E = 2.423 \text{ V} \quad (10)$$

Figure 5. The schematic working mechanism of dual/amphoteric electrolyte Zn-MnO$_2$ batteries.

　　　The increased theoretical battery potential and widened water decomposition window can also be explained with Pourbaix diagrams. As shown in Figure 6, by operating the battery in a constant pH electrolyte, the maximum water–electrolyte operation potential window is ~1.23 V. By operating a water-based electrolyte battery in a wider potential window, oxygen evolution reaction (OER) and hydrogen evolution reaction (HER) can take place. If a dual-electrolyte system is used and the cathode is operated at lower pH values and the anode at higher pH values, as shown in Figure 6, the stable electrochemical window of water could be increased to ~2 V. However, the HER has a high overpotential for zinc, which can be explained by the Tafel Equation (11):

$$\eta = \alpha + b \log i \tag{11}$$

where η is the HER overpotential, α is the transfer coefficient (overpotential when current density i is equal to the unit current density), b is the Tafel slope (a constant), and i is the current density [60,61]. In addition, OER has a significant intrinsic overpotential of at least 0.37 V due to the complex reaction mechanism [62] and slow reaction kinetics [63]. This way, the water–electrolyte operating potential significantly improves up to 3 V, and the OER and HER reactions are prohibited, thus paving the way for high-voltage aqueous batteries.

　　　Overall, this idea of creating electrolytes with different pH values and increasing the supposed half-reaction potentials as well as the origin of the water decomposition potential origin can be found described in 2005 by three non-related articles. S. Hasegawa with co-authors [64] demonstrated an H$_2$O$_2$ fuel cell with acidic (H$_2$SO$_4$) catholyte and alkaline (NaOH) anolyte. J.L. Cohen with co-authors [65] published findings on H$_2$/O$_2$ fuel cells, where acidic (0.1 M H$_2$SO$_4$) and alkaline (0.1 M KOH) electrolytes were used. Additionally, in the same year, E.R. Choban with co-authors [66] presented a methanol/O$_2$ fuel cell with acidic (0.5 M H$_2$SO$_4$) and alkaline (1 M KOH) electrolytes. Later this dual-electrolyte (acidic and alkaline) idea was adapted to different electrode batteries such as Al-air [67–70], Zn-air [68,71,72], Mg-air [68,73], Zn-PbO$_2$ [74–76], Zn-Br$_2$ [77], etc. However, the battery working time and efficiency of this battery cell type are limited by both the electrolyte

neutralization reaction and ion diffusion. Scientists have tried to overcome this limitation by using membranes and/or gelation of electrolytes.
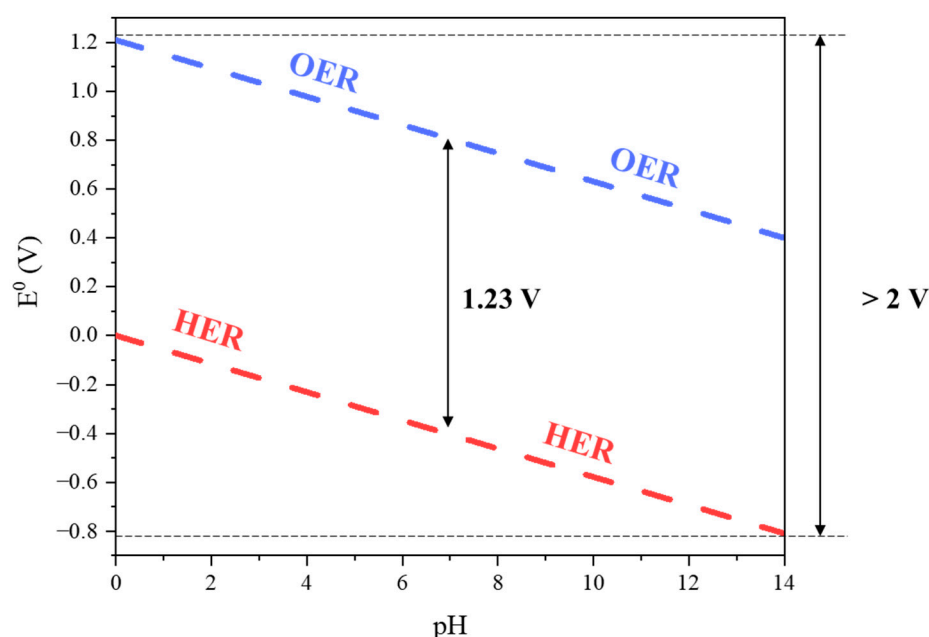

Figure 6. Pourbaix diagram of water.

The first zinc–manganese compound-based battery using an acid-alkaline dual electrolyte was presented by L. Chen with co-authors [78]. The battery cell consisted of a Zn metal sheet placed in an alkaline anolyte (KOH + LiOH solution) against Ti mesh (current collector) placed in an acidic $KMnO_4$ (active cathode material) catholyte. The battery exhibited an astonishing OCP of 2.8 V and a capacity of up to 750 mAh/g (discharge current density of 375 mA/g). However, no charge–discharge cycles were observed. Later, G. G. Yadav with co-authors [79] showed a two-compartment $Zn-MnO_2$ cell in 2019. The Zn anode compartment electrolyte consisted of a 45% KOH aqueous solution gelled in potassium polyacrylate. The MnO_2 cathode compartment electrolyte consisted of either $KMnO_4$ or $MnSO_4$ in a diluted H_2SO_4 solution. Both compartments were separated using a cellophane membrane, as shown in Figure 7a. This approach enabled achieving cell potential up to 2.45 V ($MnSO_4$) and 2.8 V ($KMnO_4$). Battery cells with $KMnO_4$ in the catholyte were stable, with capacity retention for 35 charge/discharge cycles when utilized at 20% (~62 mAh/g) of MnO_2 one-electron capacity. Moreover, the battery cells with $MnSO_4$ in the catholyte were stable for 120 charge/discharge cycles when utilized at a capacity of 20% (~62 mAh/g). Unfortunately, this article does not present measurements that would exceed the 35 h mark. A similar approach to $Zn-MnO_2$ cells has been shown by C. Liu with co-authors [80] in 2020. As depicted in Figure 7b, the cell consisted of two electrolyte compartments: 2.4 M KOH + 0.1 M $Zn(CH_3COO)_2$ anolyte and 0.5 M H_2SO_4 + 1.0 M $MnSO_4$ catholyte. A bipolar membrane was used to prevent ion migration. With this design, a cell potential of ~2.4 V was demonstrated, a Coulombic efficiency of 98.4% was reached, and 1500 cycles were performed while utilizing 0.4 mAh/cm^{-2} areal capacity.

Other authors have tried to improve this concept by adding one more (neutral) compartment between the alkaline and acidic electrolytes. C. Zhong with co-authors [32] in 2020 showed a rechargeable $Zn-MnO_2$ battery as shown in Figure 7c. The battery cell consisted of three electrolyte compartments: (1) acidic 3M H_2SO_4 + 0.1 M $MnSO_4$ catholyte; (2) neutral 0.1 M K_2SO_4 electrolyte; (3) alkaline 6 M KOH + 0.2 M ZnO + 5 mM vanillin anolyte. The acidic and alkaline compartments were separated from the neutral compartment using anion- and cation-exchange membranes. In this system, an astonishing OCP of 2.83 V was recorded. Additionally, deep discharge (616 mAh/g) cycling was performed

for over 200 h, with 2% capacity fading. However, it should be noted that ion-selective membranes are quite expensive.
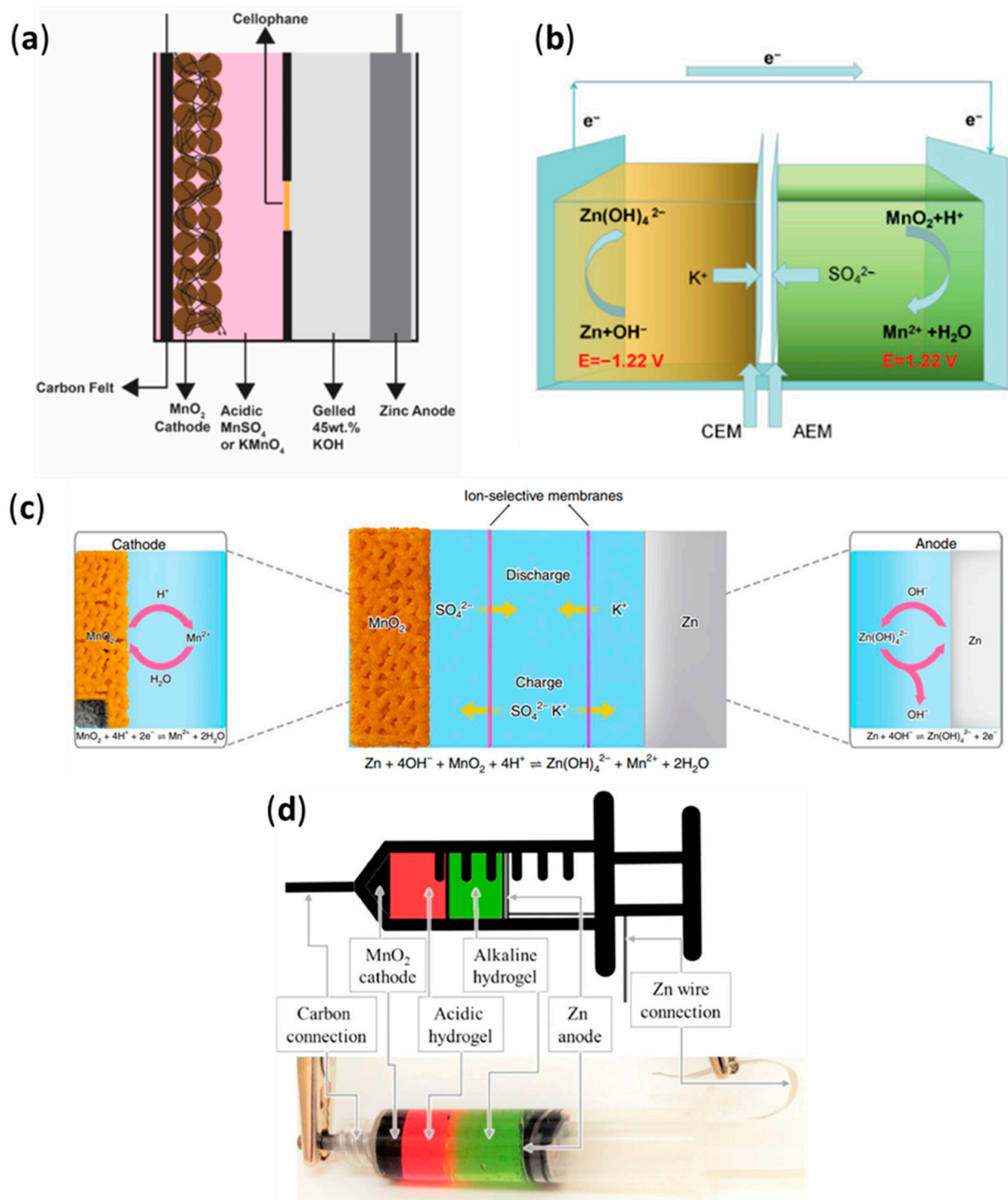
Figure 7. Design schemes of different aqueous amphoteric (dual) electrolyte Zn-MnO$_2$ batteries: (**a**) experimental setup of G. G. Yadav (Reprinted with permission from Ref. [79]. Copyright 2019 American Chemical Society.); (**b**) experimental setup of C. Liu (Reproduced with permission from Ref. [80]; published by John Wiley & Sons, Inc., Hoboken, NJ, USA, 2020); (**c**) experimental setup of C. Zhong (Reproduced with permission from Ref. [32]; published by Springer Nature Limited, 2020); (**d**) experimental setup of A. Zukuls (Reproduced with permission from Ref. [59]; published by Elsevier B.V, 2022).

More recently, in 2022, A. Zukuls with co-authors [59] demonstrated a rechargeable aqueous Zn-MnO_2 battery in which the mixing of anolyte and catholyte was prevented by gelling both electrolytes. As shown in Figure 7d, the battery consisted of an acidic (0.5 M H_2SO_4) Pluronic® F-127 aqueous catholyte and an alkaline (1.0 M KOH) Pluronic® F-127 aqueous anolyte. No specific membranes were used in this design, only a porous paper separator was used for visual purposes. With this design, 200 charge–discharge cycles were performed (cycling ~10% of MnO_2 one-electron capacity) while maintaining a high and stable OCP of ~2.4 V. Additionally, the impact of a neutral layer (0.5 M K_2SO_4 + Pluronic® F-127) between the catholyte and anolyte was tested. With this configuration, 200 cycles (cycling ~10% of MnO_2 one-electron capacity) were also performed while maintaining a high and stable OCP of ~2.4 V. However, the discharge and charge potentials were 0.5 V lower and higher, respectively. Although in the design with the neutral layer, a larger internal resistance was observed due to an increase and decrease in the charge–discharge potential, the battery was overall more stable. In a two-layer electrolyte, the battery was stable only for 25 h; however, in a three-layer electrolyte, the battery was stable for 30 h. After this time, a rapid neutralization reaction took place and battery failure was observed. Even though this battery design did not use expensive ion-exchange membranes, thus reducing the expected price, the design did not provide long-term use. Other studies describing zinc–manganese compound-based batteries with dual (amphoteric) electrolytes are listed in Table 1.

Table 1. List of papers investigating zinc–manganese compound-based batteries with dual electrolytes.

Ref.	Year of Publishing	Anode Material	Cathode Material	Anolyte	Catholyte	Membrane	Potential	Cycling	Maximum Capacity	Capacity Retention	Stability
[78]	2013	Zn-plate	$KMnO_4$ dissolved in catholyte (Ti mesh as a current collector)	2 M KOH + 2 M LiOH	1 M H_2SO_4 + $KMnO_4$	Li-ion exchange membrane ($Li_{1+x+y}Al_xTi_{2-x}Si_yP_{3-y}O_{12}$)	2.8 V OCP	-	from 510 mAh/g (discharge current density of 37.5 mA/g) to 750 mAh/g (discharge current density of 375 mA/g)	-	~110 h (with an intermittent supply of $KMnO_4$)
[79]	2019	Zn-foil	85 wt% electrolytic manganese dioxide + 15 wt% multiwalled carbon nanotubes on carbon felt	~45 wt% KOH solution in potassium polyacrylate	1 M $MnSO_4$ + 0.5 M H_2SO_4 mixed in ratio of 4:1	Four-layers of cellophane	2.45 OCP	120 cycles (capacity 62 mAh/g) at C/2	308 mAh/g at C/2	100%	35 h
		Zn-foil	85 wt% electrolytic manganese dioxide + 15 wt% multiwalled carbon nanotubes on carbon felt	~45 wt% KOH solution in potassium polyacrylate	1 M $MnSO_4$ + 0.5 M H_2SO_4 mixed in ratio of 1:3	Four-layers of cellophane	2.8 OCP	35 cycles (capacity 62 mAh/g) at C/2	308 mAh/g at C/2	100%	35 h
[80]	2020	Zn-foil	potentiostatic electrodeposited MnO_2 on carbon cloth	2.4 M KOH + 0.1 M $Zn(CH_3COO)$	0.5 M H_2SO_4 + 1.0 M $MnSO_4$	bipolar membrane (Fumasep FBM)	2.42 V at 2 mA/cm^2	1500 cycles (capacity of 0.4 mAh/cm^2) at the current density of 2 mA/cm^2	0.4 mAh/cm^2 at the current density of 2 mA/cm^2	~90%	200 h

Table 1. *Cont.*

Ref.	Year of Publishing	Anode Material	Cathode Material	Anolyte	Catholyte	Membrane	Potential	Cycling	Maximum Capacity	Capacity Retention	Stability
[58]	2020	Zn-foil	carbon-felt as a cathode-less current-collector	3 M NaOH + 0.3 M ZnO	3 M MnSO$_4$ + 0.3 M H$_2$SO$_4$ + 0.06 M NiSO$_4$	Selective membrane (no more information provided)	2.44 at 1 mA/cm (1C)	450 cycles (capacity of 1.0 mAh/cm^2) at 2C	1.0 mAh/cm^2 (or ~270 mAh/g) at 1C	99.9%	140 h
[81]	2020	Zn-foil	MnO$_2$ + acetylene black + PTFE (70:20:10)	1 M NaOH + 0.01 M Zn(CH$_3$CO$_2$)$_2$	2 M ZnSO$_4$ + 0.1 M MnSO$_4$	Nafion 115	2.2 V	90 cycles (capacity 282.2–428.6 mAh/g) at 200 mA/g	300 mAh/g at (not specified)	~100%	Not shown
[82]	2021	Zn-foil	MnO$_2$ powder coated on Ti foil	2 M ZnSO$_4$ + H$_2$SO$_4$ gelled in polyacrylamide	2 M ZnSO$_4$ (with adjusted pH = 7) gelled in polyacrylamide	Neutral layer: 2 M Zn$_5$O$_4$ gelled in sodium polyacrylate	1.8 V at 5 A/g	5000 cycles (capacity of 150 mAh/g) at 5 A/g	516 mAh/g at 0.05 A/g	93.18%	>6 months
[59]	2022	Zn-foil	MnO$_2$ + carbon black (13:5) on carbon felt	1 M KOH Pluronic® F-127 hydrogel	0.5 M H$_2$SO$_4$ Pluronic® F-127 hydrogel	-	2.4 V OCP	200 cycles (discharge for 120 s) at 1 mA/s	25 mAh/g at 20 mA/g	-	>25 h
[83]	2022	Zn-foil	MoS-MnO$_2$ heterostructure + conductive carbon + PVDF (80:15:5) on carbon cloth	1 M Zn(ClO$_4$)$_2$ + acetonitrile + water + H$_2$SO$_4$	1 M Zn(ClO$_4$)$_2$ + acetonitrile + water + KOH	PVA+PVP crosslinked membrane	1.9 V (at the start of discharge at 0.2 A/g)	5000 cycles (160 mAh/g) at 10 A/g	464 mAh/g at 0.2 A/g	74%	Not shown
[84]	2022	Zn-foil	potentiostatic electrodeposited MnO$_2$ from catholyte on carbon cloth	0.3 M ZnO + 3 M NaOH	3 M MnSO$_4$ + 0.3 M H$_2$SO$_4$	agar with Na$_2$SO$_4$	2.5 V at 0.1 C	350 cycles (capacity ~550 mAh/g) at 1 C	577.8 mAh/g at 1C	94%	>350 h

Table 1. *Cont.*

Ref.	Year of Publishing	Anode Material	Cathode Material	Anolyte	Catholyte	Membrane	Potential	Cycling	Maximum Capacity	Capacity Retention	Stability
[85]	2022	Zn-foil	electrochemically deposited MnO_2 on carbon paper	0.5 M $ZnSO_4$ + 1 M LiTFSI (bis(trifluoro methane)sulf onimide lithium salt)	1 M $MnSO_4$ + 1 M HTFSI (bis(trifluoro methanesulfo nyl)imide)	dual-hydrophobic-induced membrane (consisting of polymer/ionic liq-uid/graphene mixture)	2.05 V at 1 mA/cm	2000 cycles (fixed area capacity of 1 mAh/cm^2) at 1 mA/cm^2	18 mAh/cm^2 at 1 mA/cm^2	98%	2275 h
[86]	2023	Zn-foil	carbon cloth	2.4 M KOH + 0.1 M $Zn(CH_3COO)_2$	1.0 M H2SO4 + 0.3 M CuSO4 + 1.0 M MnSO4	Cu foil	1.84 V at 2.5 mA/cm^2	3500 (capacity ~0.5 mAh/cm^2) at 2.5 mA/cm^2	0.5 mAh/cm^2 at 2.5 mA/cm^2	~125% (Coulombic efficiency after 3500 cycles)	>107 h

5. Challenges and Outlook

Primary aqueous alkaline Zn-MnO$_2$ battery technology already dominates the primary battery market. This technology has proven itself as safe, affordable, and reliable. As the world moves towards renewable energy sources, we are in need of safe, affordable, and reliable secondary battery technology with a high-power density and excellent capacity retention during charge/discharge cycles. A good candidate for this application could be aqueous Zn-MnO$_2$ battery technology. However, several improvements and new technological approaches are needed. A very new approach has been demonstrated by G. G. Yadav with co-authors [79] and by others [32,59,80]. In the literature, dual (amphoteric) electrolyte aqueous cells have been demonstrated that result in a significant increase in cell potential over 2 V. This voltage increase has been achieved in these new aqueous cell types by placing a Zn anode in an alkaline medium and an MnO$_2$ cathode in an acidic medium. To prevent neutralization reactions from occurring, different approaches have been used, such as the usage of ion exchange membranes or other types of membranes, gelation of electrolytes, or both. However, when put to the test, this cell design presents several problems that should be addressed in the near future by researchers. Different recyclability problems continue to exist for the Zn anode in an alkaline medium and the MnO$_2$ cathode in an acidic medium. For aqueous Zn-MnO$_2$ batteries to compete with LIBs, full utilization of the MnO$_2$ cathode capacity should be achieved with high-capacity retention over a large number of charge–discharge cycles. Additionally, the economic aspects should be taken into account when considering new types of chemical energy storage systems. Although ion exchange membranes provide excellent immiscibility with the electrolyte pH, they are quite expensive. Different hydrogels such as Pluronic$^®$ F-127 are economically disadvantageous as well. Thus, effective methods for pH immobilization should be more thoughtfully considered.

6. Conclusions

In this short review, aqueous Zn-MnO$_2$ batteries with different pH electrolytes have been acknowledged. The historical origins of alkaline Zn-MnO$_2$ batteries can be traced back to the middle of the 20th century. Although they have been successfully utilized in the primary battery market and research has been carried out to tackle the rechargeability challenges, little to no secondary aqueous Zn-MnO$_2$ batteries are seen in the market. Another type of Zn-MnO$_2$ battery discussed is a mild to acidic aqueous electrolyte battery. If an alkaline-type battery suffers from electrochemically inactive and insoluble compound formations, such as Mn$_3$O$_4$ and ZnMn$_2$O$_4$, then, in an acidic electrolyte, this problem is partially solved since these compounds are soluble in acid. Moreover, by decreasing the pH value of the electrolyte, the cathode goes through a higher potential reaction and increases the overall potential of the cell from 1.4–1.6 V in the alkaline electrolyte to 1.9–2.0 V in the mild/acidic electrolyte. However, more recently, the scientific community has shown a new and innovative battery cell type that combines the positive effects of alkaline and acidic electrolytes and advances the possibility of creating a water-electrolyte battery with a potential of up to 3 V. This has been accomplished by operating the anode in an alkaline medium and cathode in an acidic medium. Thus, increasing the potential of this aqueous dual/amphoteric electrolyte Zn-MnO$_2$ battery up to 2.4 V improves the reachability of the cell. However, this unique battery cell imposes new challenges, such as neutralization reactions between both electrolytes.

Institutional Review Board Statement: Not applicable.

Informed Consent Statement: Not applicable.

Data Availability Statement: Not applicable.

Conflicts of Interest: The authors declare that they have no known competing financial interests or personal relationships that could have appeared to influence the work reported in this paper.

References

1. Collins, J.; Gourdin, G.; Qu, D. Modern Applications of Green Chemistry. In *Green Chemistry*; Elsevier: Amsterdam, The Netherlands, 2018; pp. 771–860.
2. Ziegler, M.S.; Mueller, J.M.; Pereira, G.D.; Song, J.; Ferrara, M.; Chiang, Y.-M.; Trancik, J.E. Storage Requirements and Costs of Shaping Renewable Energy Toward Grid Decarbonization. *Joule* **2019**, *3*, 2134–2153. [CrossRef]
3. Lu, L.; Han, X.; Li, J.; Hua, J.; Ouyang, M. A Review on the Key Issues for Lithium-Ion Battery Management in Electric Vehicles. *J. Power Sources* **2013**, *226*, 272–288. [CrossRef]
4. Chen, Y.; Kang, Y.; Zhao, Y.; Wang, L.; Liu, J.; Li, Y.; Liang, Z.; He, X.; Li, X.; Tavajohi, N.; et al. A Review of Lithium-Ion Battery Safety Concerns: The Issues, Strategies, and Testing Standards. *J. Energy Chem.* **2021**, *59*, 83–99. [CrossRef]
5. Galushkin, N.E.; Yazvinskaya, N.N.; Galushkin, D.N. Mechanism of Thermal Runaway in Lithium-Ion Cells. *J. Electrochem. Soc.* **2018**, *165*, A1303–A1308. [CrossRef]
6. Yang, J.; Liu, X.; Tian, J.; Ma, X.; Wang, B.; Li, W.; Wang, Q. Adhesive Nanocomposites of Hypergravity Induced Co_3O_4 Nanoparticles and Natural Gels as Li-Ion Battery Anode Materials with High Capacitance and Low Resistance. *RSC Adv.* **2017**, *7*, 21061–21067. [CrossRef]
7. Lim, M.B.; Lambert, T.N.; Chalamala, B.R. Rechargeable Alkaline Zinc–Manganese Oxide Batteries for Grid Storage: Mechanisms, Challenges and Developments. *Mater. Sci. Eng. R Rep.* **2021**, *143*, 100593. [CrossRef]
8. Park, J.; Kim, M.; Choi, J.; Lee, S.; Kim, J.; Han, D.; Jang, H.; Park, M. Recent Progress in High-voltage Aqueous Zinc-based Hybrid Redox Flow Batteries. *Chem. Asian J.* **2023**, *18*, e202201052. [CrossRef]
9. Seong, W.M.; Park, K.-Y.; Lee, M.H.; Moon, S.; Oh, K.; Park, H.; Lee, S.; Kang, K. Abnormal Self-Discharge in Lithium-Ion Batteries. *Energy Environ. Sci.* **2018**, *11*, 970–978. [CrossRef]
10. Duh, Y.S.; Lin, K.H.; Kao, C.S. Experimental Investigation and Visualization on Thermal Runaway of Hard Prismatic Lithium-Ion Batteries Used in Smart Phones. *J. Therm. Anal. Calorim.* **2018**, *132*, 1677–1692. [CrossRef]
11. Nitta, N.; Wu, F.; Lee, J.T.; Yushin, G. Li-Ion Battery Materials: Present and Future. *Mater. Today* **2015**, *18*, 252–264. [CrossRef]
12. Zaman, W.; Hatzell, K.B. Processing and Manufacturing of next Generation Lithium-Based All Solid-State Batteries. *Curr. Opin. Solid State Mater. Sci.* **2022**, *26*, 101003. [CrossRef]
13. Wang, H.; Shi, W.; Hu, F.; Wang, Y.; Hu, X.; Li, H. Over-Heating Triggered Thermal Runaway Behavior for Lithium-Ion Battery with High Nickel Content in Positive Electrode. *Energy* **2021**, *224*, 120072. [CrossRef]
14. Chen, S.; Gao, Z.; Sun, T. Safety Challenges and Safety Measures of Li-Ion Batteries. *Energy Sci. Eng.* **2021**, *9*, 1647–1672. [CrossRef]
15. Zeng, A.; Chen, W.; Rasmussen, K.D.; Zhu, X.; Lundhaug, M.; Müller, D.B.; Tan, J.; Keiding, J.K.; Liu, L.; Dai, T.; et al. Battery Technology and Recycling Alone Will Not Save the Electric Mobility Transition from Future Cobalt Shortages. *Nat. Commun.* **2022**, *13*, 1341. [CrossRef]
16. Zhang, J.; Lei, Y.; Lin, Z.; Xie, P.; Lu, H.; Xu, J. A Novel Approach to Recovery of Lithium Element and Production of Holey Graphene Based on the Lithiated Graphite of Spent Lithium Ion Batteries. *Chem. Eng. J.* **2022**, *436*, 135011. [CrossRef]
17. Liu, B.; Zhang, Q.; Liu, J.; Hao, Y.; Tang, Y.; Li, Y. The Impacts of Critical Metal Shortage on China's Electric Vehicle Industry Development and Countermeasure Policies. *Energy* **2022**, *248*, 123646. [CrossRef]
18. Zhang, H.; Lu, W.; Li, X. Progress and Perspectives of Flow Battery Technologies. *Electrochem. Energy Rev.* **2019**, *2*, 492–506. [CrossRef]
19. Luo, H.; Liu, B.; Yang, Z.; Wan, Y.; Zhong, C. The Trade-Offs in the Design of Reversible Zinc Anodes for Secondary Alkaline Batteries. *Electrochem. Energy Rev.* **2022**, *5*, 187–210. [CrossRef]
20. Yadav, G.G.; Wei, X.; Huang, J.; Turney, D.; Nyce, M.; Banerjee, S. Accessing the Second Electron Capacity of MnO_2 by Exploring Complexation and Intercalation Reactions in Energy Dense Alkaline Batteries. *Int. J. Hydrogen Energy* **2018**, *43*, 8480–8487. [CrossRef]
21. Placke, T.; Kloepsch, R.; Dühnen, S.; Winter, M. Lithium Ion, Lithium Metal, and Alternative Rechargeable Battery Technologies: The Odyssey for High Energy Density. *J. Solid State Electrochem.* **2017**, *21*, 1939–1964. [CrossRef]
22. Shin, J.; Seo, J.K.; Yaylian, R.; Huang, A.; Meng, Y.S. A Review on Mechanistic Understanding of MnO_2 in Aqueous Electrolyte for Electrical Energy Storage Systems. *Int. Mater. Rev.* **2020**, *65*, 356–387. [CrossRef]

23. Akinyele, D.; Belikov, J.; Levron, Y. Battery Storage Technologies for Electrical Applications: Impact in Stand-Alone Photovoltaic Systems. *Energies* **2017**, *10*, 1760. [CrossRef]
24. Song, J.; Xu, K.; Liu, N.; Reed, D.; Li, X. Crossroads in the Renaissance of Rechargeable Aqueous Zinc Batteries. *Mater. Today* **2021**, *45*, 191–212. [CrossRef]
25. Takamura, T. PRIMARY BATTERIES—AQUEOUS SYSTEMS | Alkaline Manganese–Zinc. In *Encyclopedia of Electrochemical Power Sources*; Elsevier: Amsterdam, The Netherlands, 2009; pp. 28–42.
26. Owens, B.B.; Reale, P.; Scrosati, B. PRIMARY BATTERIES | Overview. In *Encyclopedia of Electrochemical Power Sources*; Elsevier: Amsterdam, The Netherlands, 2009; pp. 22–27.
27. D'Ambrose, M.J.; Turney, D.E.; Yadav, G.G.; Nyce, M.; Banerjee, S. Material Failure Mechanisms of Alkaline Zn Rechargeable Conversion Electrodes. *ACS Appl. Energy Mater.* **2021**, *4*, 3381–3392. [CrossRef]
28. Yadav, G.G.; Gallaway, J.W.; Turney, D.E.; Nyce, M.; Huang, J.; Wei, X.; Banerjee, S. Regenerable Cu-Intercalated MnO_2 Layered Cathode for Highly Cyclable Energy Dense Batteries. *Nat. Commun.* **2017**, *8*, 14424. [CrossRef] [PubMed]
29. Liu, X.; Yi, J.; Wu, K.; Jiang, Y.; Liu, Y.; Zhao, B.; Li, W.; Zhang, J. Rechargeable Zn–MnO_2 Batteries: Advances, Challenges and Perspectives. *Nanotechnology* **2020**, *31*, 122001. [CrossRef] [PubMed]
30. Faegh, E.; Omasta, T.; Hull, M.; Ferrin, S.; Shrestha, S.; Lechman, J.; Bolintineanu, D.; Zuraw, M.; Mustain, W.E. Understanding the Dynamics of Primary Zn-MnO_2 Alkaline Battery Gassing with Operando Visualization and Pressure Cells. *J. Electrochem. Soc.* **2018**, *165*, A2528–A2535. [CrossRef]
31. Perez-Antolin, D.; Sáez-Bernal, I.; Colina, A.; Ventosa, E. Float-Charging Protocol in Rechargeable Zn–MnO_2 Batteries: Unraveling the Key Role of Mn^{2+} Additives in Preventing Spontaneous PH Changes. *Electrochem. Commun.* **2022**, *138*, 107271. [CrossRef]
32. Zhong, C.; Liu, B.; Ding, J.; Liu, X.; Zhong, Y.; Li, Y.; Sun, C.; Han, X.; Deng, Y.; Zhao, N.; et al. Decoupling Electrolytes towards Stable and High-Energy Rechargeable Aqueous Zinc–Manganese Dioxide Batteries. *Nat. Energy* **2020**, *5*, 440–449. [CrossRef]
33. Bai, L.; Qu, D.Y.; Conway, B.E.; Zhou, Y.H.; Chowdhury, G.; Adams, W.A. Rechargeability of a Chemically Modified MnO_2/Zn Battery System at Practically Favorable Power Levels. *J. Electrochem. Soc.* **1993**, *140*, 884–889. [CrossRef]
34. Hertzberg, B.J.; Huang, A.; Hsieh, A.; Chamoun, M.; Davies, G.; Seo, J.K.; Zhong, Z.; Croft, M.; Erdonmez, C.; Meng, Y.S.; et al. Effect of Multiple Cation Electrolyte Mixtures on Rechargeable Zn–MnO_2 Alkaline Battery. *Chem. Mater.* **2016**, *28*, 4536–4545. [CrossRef]
35. Ingale, N.D.; Gallaway, J.W.; Nyce, M.; Couzis, A.; Banerjee, S. Rechargeability and Economic Aspects of Alkaline Zinc-Manganese Dioxide Cells for Electrical Storage and Load Leveling. *J. Power Sources* **2015**, *276*, 7–18. [CrossRef]
36. Bruck, A.M.; Kim, M.A.; Ma, L.; Ehrlich, S.N.; Okasinski, J.S.; Gallaway, J.W. Bismuth Enables the Formation of Disordered Birnessite in Rechargeable Alkaline Batteries. *J. Electrochem. Soc.* **2020**, *167*, 110514. [CrossRef]
37. Rus, E.D.; Moon, G.D.; Bai, J.; Steingart, D.A.; Erdonmez, C.K. Electrochemical Behavior of Electrolytic Manganese Dioxide in Aqueous KOH and LiOH Solutions: A Comparative Study. *J. Electrochem. Soc.* **2016**, *163*, A356–A363. [CrossRef]
38. Kelly, M.; Duay, J.; Lambert, T.N.; Aidun, R. Impact of Triethanolamine as an Additive for Rechargeable Alkaline Zn/MnO_2 Batteries under Limited Depth of Discharge Conditions. *J. Electrochem. Soc.* **2017**, *164*, A3684–A3691. [CrossRef]
39. Minakshi, M.; Singh, P. Synergistic Effect of Additives on Electrochemical Properties of MnO_2 Cathode in Aqueous Rechargeable Batteries. *J. Solid State Electrochem.* **2012**, *16*, 1487–1492. [CrossRef]
40. Poosapati, A.; Vadnala, S.; Negrete, K.; Lan, Y.; Hutchison, J.; Zupan, M.; Madan, D. Rechargeable Zinc-Electrolytic Manganese Dioxide (EMD) Battery with a Flexible Chitosan-Alkaline Electrolyte. *ACS Appl. Energy Mater.* **2021**, *4*, 4248–4258. [CrossRef]
41. Minakshi, M.; Ralph, D. A Novel Sodium-Ion Rechargeable Battery. *ECS Trans.* **2013**, *45*, 95–102. [CrossRef]
42. Wei, Z.; Cheng, J.; Wang, R.; Li, Y.; Ren, Y. From Spent Zn–MnO_2 Primary Batteries to Rechargeable Zn–MnO_2 Batteries: A Novel Directly Recycling Route with High Battery Performance. *J. Environ. Manag.* **2021**, *298*, 113473. [CrossRef]
43. Soundharrajan, V.; Sambandam, B.; Kim, S.; Islam, S.; Jo, J.; Kim, S.; Mathew, V.; Sun, Y.; Kim, J. The Dominant Role of Mn^{2+} Additive on the Electrochemical Reaction in $ZnMn_2O_4$ Cathode for Aqueous Zinc-Ion Batteries. *Energy Storage Mater.* **2020**, *28*, 407–417. [CrossRef]
44. Wang, C.; Zeng, Y.; Xiao, X.; Wu, S.; Zhong, G.; Xu, K.; Wei, Z.; Su, W.; Lu, X. γ-MnO_2 Nanorods/Graphene Composite as Efficient Cathode for Advanced Rechargeable Aqueous Zinc-Ion Battery. *J. Energy Chem.* **2020**, *43*, 182–187. [CrossRef]
45. Lee, J.-W.; Seo, S.-D.; Kim, D.-W. Comparative Study on Ternary Spinel Cathode Zn–Mn–O Microspheres for Aqueous Rechargeable Zinc-Ion Batteries. *J. Alloy. Compd.* **2019**, *800*, 478–482. [CrossRef]
46. Xu, D.; Li, B.; Wei, C.; He, Y.-B.; Du, H.; Chu, X.; Qin, X.; Yang, Q.-H.; Kang, F. Preparation and Characterization of MnO_2/Acid-Treated CNT Nanocomposites for Energy Storage with Zinc Ions. *Electrochim. Acta* **2014**, *133*, 254–261. [CrossRef]
47. Han, K.; An, F.; Yan, F.; Chen, H.; Wan, Q.; Liu, Y.; Li, P.; Qu, X. High-Performance Aqueous Zn–MnO_2 Batteries Enabled by the Coupling Engineering of K^+ Pre-Intercalation and Oxygen Defects. *J. Mater. Chem. A Mater.* **2021**, *9*, 15637–15647. [CrossRef]
48. Chao, D.; Zhou, W.; Ye, C.; Zhang, Q.; Chen, Y.; Gu, L.; Davey, K.; Qiao, S. An Electrolytic Zn–MnO_2 Battery for High-Voltage and Scalable Energy Storage. *Angew. Chem. Int. Ed.* **2019**, *58*, 7823–7828. [CrossRef]
49. Kim, S.J.; Wu, D.; Housel, L.M.; Wu, L.; Takeuchi, K.J.; Marschilok, A.C.; Takeuchi, E.S.; Zhu, Y. Toward the Understanding of the Reaction Mechanism of Zn/MnO_2 Batteries Using Non-Alkaline Aqueous Electrolytes. *Chem. Mater.* **2021**, *33*, 7283–7289. [CrossRef]
50. Boytsova, O.V.; Shekunova, T.O.; Baranchikov, A.E. Nanocrystalline Manganese Dioxide Synthesis by Microwave-Hydrothermal Treatment. *Russ. J. Inorg. Chem.* **2015**, *60*, 546–551. [CrossRef]

51. Krężel, A.; Maret, W. The Biological Inorganic Chemistry of Zinc Ions. *Arch. Biochem. Biophys.* **2016**, *611*, 3–19. [CrossRef]

52. Wang, M.; Zheng, X.; Zhang, X.; Chao, D.; Qiao, S.; Alshareef, H.N.; Cui, Y.; Chen, W. Opportunities of Aqueous Manganese-Based Batteries with Deposition and Stripping Chemistry. *Adv. Energy Mater.* **2021**, *11*, 2002904. [CrossRef]

53. Yang, J.; Cao, J.; Peng, Y.; Yang, W.; Barg, S.; Liu, Z.; Kinloch, I.A.; Bissett, M.A.; Dryfe, R.A.W. Unravelling the Mechanism of Rechargeable Aqueous Zn–MnO$_2$ Batteries: Implementation of Charging Process by Electrodeposition of MnO$_2$. *ChemSusChem* **2020**, *13*, 4103–4110. [CrossRef]

54. Mitha, A.; Mi, H.; Dong, W.; Cho, I.S.; Ly, J.; Yoo, S.; Bang, S.; Hoang, T.K.A.; Chen, P. Thixotropic Gel Electrolyte Containing Poly(Ethylene Glycol) with High Zinc Ion Concentration for the Secondary Aqueous Zn/LiMn$_2$O$_4$ Battery. *J. Electroanal. Chem.* **2019**, *836*, 1–6. [CrossRef]

55. Pan, H.; Shao, Y.; Yan, P.; Cheng, Y.; Han, K.S.; Nie, Z.; Wang, C.; Yang, J.; Li, X.; Bhattacharya, P.; et al. Reversible Aqueous Zinc/Manganese Oxide Energy Storage from Conversion Reactions. *Nat. Energy* **2016**, *1*, 16039. [CrossRef]

56. Qiu, C.; Zhu, X.; Xue, L.; Ni, M.; Zhao, Y.; Liu, B.; Xia, H. The Function of Mn^{2+} Additive in Aqueous Electrolyte for Zn/δ-MnO$_2$ Battery. *Electrochim. Acta* **2020**, *351*, 136445. [CrossRef]

57. Demir-Cakan, R.; Palacin, M.R.; Croguennec, L. Rechargeable Aqueous Electrolyte Batteries: From Univalent to Multivalent Cation Chemistry. *J. Mater. Chem. A Mater.* **2019**, *7*, 20519–20539. [CrossRef]

58. Chao, D.; Ye, C.; Xie, F.; Zhou, W.; Zhang, Q.; Gu, Q.; Davey, K.; Gu, L.; Qiao, S. Atomic Engineering Catalyzed MnO$_2$ Electrolysis Kinetics for a Hybrid Aqueous Battery with High Power and Energy Density. *Adv. Mater.* **2020**, *32*, 2001894. [CrossRef]

59. Dūrena, R.; Zukuls, A.; Vanags, M.; Šutka, A. How to Increase the Potential of Aqueous Zn-MnO$_2$ Batteries: The Effect of PH Gradient Electrolyte. *Electrochim. Acta* **2022**, *434*, 141275. [CrossRef]

60. Li, C.; Xie, X.; Liang, S.; Zhou, J. Issues and Future Perspective on Zinc Metal Anode for Rechargeable Aqueous Zinc-ion Batteries. *Energy Environ. Mater.* **2020**, *3*, 146–159. [CrossRef]

61. Ibrahim, M.A. Improving the Throwing Power of Acidic Zinc Sulfate Electroplating Baths. *J. Chem. Technol. Biotechnol.* **2000**, *75*, 745–755. [CrossRef]

62. Li, J. Oxygen Evolution Reaction in Energy Conversion and Storage: Design Strategies Under and Beyond the Energy Scaling Relationship. *Nanomicro. Lett.* **2022**, *14*, 112. [CrossRef]

63. Zhang, G.-R.; Shen, L.-L.; Mei, D. Enhanced Electrocatalysis at Ionic Liquid Modified Solid–Liquid Interfaces. In *Reference Module in Chemistry, Molecular Sciences and Chemical Engineering*; Elsevier: Amsterdam, The Netherlands, 2023.

64. Hasegawa, S.; Shimotani, K.; Kishi, K.; Watanabe, H. Electricity Generation from Decomposition of Hydrogen Peroxide. *Electrochem. Solid-State Lett.* **2005**, *8*, A119. [CrossRef]

65. Cohen, J.L.; Volpe, D.J.; Westly, D.A.; Pechenik, A.; Abruña, H.D. A Dual Electrolyte H$_2$/O$_2$ Planar Membraneless Microchannel Fuel Cell System with Open Circuit Potentials in Excess of 1.4 V. *Langmuir* **2005**, *21*, 3544–3550. [CrossRef] [PubMed]

66. Choban, E.R.; Spendelow, J.S.; Gancs, L.; Wieckowski, A.; Kenis, P.J.A. Membraneless Laminar Flow-Based Micro Fuel Cells Operating in Alkaline, Acidic, and Acidic/Alkaline Media. *Electrochim. Acta* **2005**, *50*, 5390–5398. [CrossRef]

67. Wen, H.; Liu, Z.; Qiao, J.; Chen, R.; Qiao, G.; Yang, J. Ultrahigh Voltage and Energy Density Aluminum-air Battery Based on Aqueous Alkaline-acid Hybrid Electrolyte. *Int. J. Energy Res.* **2020**, *44*, 10652–10661. [CrossRef]

68. Wang, Y.; Pan, W.; Luo, S.; Zhao, X.; Kwok, H.Y.H.; Xu, X.; Leung, D.Y.C. High-Performance Solid-State Metal-Air Batteries with an Innovative Dual-Gel Electrolyte. *Int. J. Hydrog. Energy.* **2022**, *47*, 15024–15034. [CrossRef]

69. Wang, L.; Cheng, R.; Liu, C.; Ma, M.C.; Wang, W.; Yang, G.; Leung, M.K.H.; Liu, F.; Feng, S.P. Trielectrolyte Aluminum-Air Cell with High Stability and Voltage beyond 2.2 V. *Mater. Today Phys.* **2020**, *14*, 100242. [CrossRef]

70. Chen, B.; Leung, D.Y.C.; Xuan, J.; Wang, H. A Mixed-PH Dual-Electrolyte Microfluidic Aluminum–Air Cell with High Performance. *Appl. Energy* **2017**, *185*, 1303–1308. [CrossRef]

71. Cai, P.; Li, Y.; Chen, J.; Jia, J.; Wang, G.; Wen, Z. An Asymmetric-Electrolyte Zn−Air Battery with Ultrahigh Power Density and Energy Density. *ChemElectroChem* **2018**, *5*, 589–592. [CrossRef]

72. Zhao, S.; Liu, T.; Dai, Y.; Wang, Y.; Guo, Z.; Zhai, S.; Yu, J.; Zhi, C.; Ni, M. All-in-One and Bipolar-Membrane-Free Acid-Alkaline Hydrogel Electrolytes for Flexible High-Voltage Zn-Air Batteries. *Chem. Eng. J.* **2022**, *430*, 132718. [CrossRef]

73. Leong, K.W.; Wang, Y.; Pan, W.; Luo, S.; Zhao, X.; Leung, D.Y.C. Doubling the Power Output of a Mg-Air Battery with an Acid-Salt Dual-Electrolyte Configuration. *J. Power Sources* **2021**, *506*, 230144. [CrossRef]

74. Xu, Y.; Cai, P.; Chen, K.; Ding, Y.; Chen, L.; Chen, W.; Wen, Z. High-Voltage Rechargeable Alkali–Acid Zn–PbO$_2$ Hybrid Battery. *Angew. Chem. Int. Ed.* **2020**, *59*, 23593–23597. [CrossRef]

75. Gao, T.; Sun, Y.; Gong, L.; Ma, C.; Wang, J.; Su, L. 2.8 V Aqueous Lead Dioxide–Zinc Rechargeable Battery Using H$_2$SO$_4$–K$_2$SO$_4$–KOH Three Electrolytes. *J. Electrochem. Soc.* **2020**, *167*, 020552. [CrossRef]

76. Wu, H.; Liu, S.-J.; Lian, K. Aqueous Based Dual-Electrolyte Rechargeable Pb–Zn Battery with a 2.8 V Operating Voltage. *J. Energy Storage* **2020**, *29*, 101305. [CrossRef]

77. Yu, F.; Pang, L.; Wang, X.; Waclawik, E.R.; Wang, F.; Ostrikov, K.; Wang, H. Aqueous Alkaline–Acid Hybrid Electrolyte for Zinc-Bromine Battery with 3V Voltage Window. *Energy Storage Mater.* **2019**, *19*, 56–61. [CrossRef]

78. Chen, L.; Guo, Z.; Xia, Y.; Wang, Y. High-Voltage Aqueous Battery Approaching 3 V Using an Acidic–Alkaline Double Electrolyte. *Chem. Commun.* **2013**, *49*, 2204. [CrossRef] [PubMed]

79. Yadav, G.G.; Turney, D.; Huang, J.; Wei, X.; Banerjee, S. Breaking the 2 V Barrier in Aqueous Zinc Chemistry: Creating 2.45 and 2.8 V MnO$_2$–Zn Aqueous Batteries. *ACS Energy Lett.* **2019**, *4*, 2144–2146. [CrossRef]

80. Liu, C.; Chi, X.; Han, Q.; Liu, Y. A High Energy Density Aqueous Battery Achieved by Dual Dissolution/Deposition Reactions Separated in Acid-Alkaline Electrolyte. *Adv Energy Mater.* **2020**, *10*, 1903589. [CrossRef]
81. Fan, W.; Liu, F.; Liu, Y.; Wu, Z.; Wang, L.; Zhang, Y.; Huang, Q.; Fu, L.; Wu, Y. A High Voltage Aqueous Zinc–Manganese Battery Using a Hybrid Alkaline-Mild Electrolyte. *Chem. Commun.* **2020**, *56*, 2039–2042. [CrossRef] [PubMed]
82. Shen, Z.; Tang, Z.; Li, C.; Luo, L.; Pu, J.; Wen, Z.; Liu, Y.; Ji, Y.; Xie, J.; Wang, L.; et al. Precise Proton Redistribution for Two-Electron Redox in Aqueous Zinc/Manganese Dioxide Batteries. *Adv Energy Mater.* **2021**, *11*, 2102055. [CrossRef]
83. Samanta, P.; Ghosh, S.; Bolar, S.; Kolya, H.; Kang, C.-W.; Samanta, P.; Chandra Murmu, N.; Kuila, T. Acid–Alkaline Electrolyte for the Development of High-Energy Density Zn-Ion Batteries through Structural Modification of MoS$_2$ by MnO$_2$. *ACS Appl. Energy Mater.* **2022**, *5*, 8581–8591. [CrossRef]
84. Xu, Q.; Xie, Q.-X.; Xue, T.; Cheng, G.; Wu, J.-D.; Ning, L.; Yan, X.-H.; Lu, Y.-J.; Zou, Z.-L.; Wang, B.-P.; et al. Salt Bridge-Intermediated Three Phase Decoupling Electrolytes for High Voltage Electrolytic Aqueous Zinc-Manganese Dioxides Battery. *Chem. Eng. J.* **2023**, *451*, 138775. [CrossRef]
85. Cui, Y.; Zhuang, Z.; Xie, Z.; Cao, R.; Hao, Q.; Zhang, N.; Liu, W.; Zhu, Y.; Huang, G. High-Energy and Long-Lived Zn–MnO$_2$ Battery Enabled by a Hydrophobic-Ion-Conducting Membrane. *ACS Nano* **2022**, *16*, 20730–20738. [CrossRef] [PubMed]
86. Liu, C.; Chi, X.; Yang, C.; Liu, Y. High-Voltage Aqueous Zinc Batteries Achieved by Tri-functional Metallic Bipolar Electrodes. *Energy Environ. Mater.* **2023**, *6*, e12300. [CrossRef]